

Ampere force based photonic crystal fiber magnetic field sensor

Sun-jie Qiu, Qi Liu, Fei Xu*, Yan-qing Lu

National Laboratory of Solid State Microstructures and College of Engineering and Applied Sciences, Nanjing University, Nanjing 210093, PR China

ARTICLE INFO

Article history:

Received 26 October 2013

Received in revised form 14 February 2014

Accepted 14 February 2014

Available online 26 February 2014

Keywords:

Ampere force

Photonic crystal fiber

Magnetic field sensor

Modal interferometer

ABSTRACT

We fabricate an Ampere force based photonic crystal fiber (PCF) magnetic field sensor by bonding a PCF in-line modal interferometer (PCFMI) with an aluminum (Al) wire together. This sensor is very compact, cost-effective, temperature insensitive, highly stable over time and easy to be fabricated only including cleaving and splicing processes. An electrical current flowing through the Al wire in a perpendicular magnetic field can generate Ampere force to lead to the curvature of the Al wire and the PCF. As the cladding mode of the PCF with a large mode field diameter is very sensitive to the curvature, the average magnetic field sensing sensitivity can reach 32.4 pm/mT when 100 mA electrical current is applied with excellent repeatability. Higher sensitivity and a minimal detectable magnetic field of less than 0.1 mT can be realized by increasing the applied electrical current.

© 2014 Elsevier B.V. All rights reserved.

1. Introduction

Fiber magnetic field sensors have been proposed for over 30 years and have always been widely studied because of their advantages such as lightweight, resistance to electromagnetic interference, small size, and capability of remote operation [1]. Much research has been concentrated on the development of magnetic field sensors utilizing Faraday effect [2,3], magnetic fluid [4–7], magnetostrictive effect [8–11], magnetic force [12] and other mechanisms. However, the magnetic field sensing sensitivities based on Faraday effect are usually very low because the Verdet constant of silica fibers is fairly small. In order to enhance the sensitivities, it normally needs to coil a long piece of fiber with multiple turns to increase the polarization rotation angle but bend-induced linear birefringence may easily affect the state of polarization and affect the measurement results [2,3]. As there exist magnetic materials, magnetic fluid [4–7], magnetostrictive effect [8–11], magnetic force [12] based magnetic field sensors have the intrinsic magnetic saturation and hysteresis effect, which will largely decrease the measurement range and cause measurement error. Recently, a novel Ampere force based magnetic field sensor has been reported, which does not have the intrinsic magnetic saturation and hysteresis effect and the sensitivity is high [13]. But their dual-polarization fiber laser beat frequency demodulating equipments are expensive and complex.

Photonic crystal fibers (PCFs), also known as microstructured optical fibers, have attracted more and more attention in the past 10 years because of their unique optical properties [14]. In recent years, PCF based in-line modal interferometers (PCFMs) built via fusion splicing has been widely investigated because of its simple fabrication and low cost [15–18]. Some research groups have also fabricated PCF based magnetic field sensors by filling magnetic fluid into the air holes of PCF [19,20]. But these magnetic fluid filled PCF magnetic field sensors also have the drawbacks of intrinsic magnetic saturation.

In this letter, we propose a novel Ampere force based PCF magnetic field sensor by bonding a PCFMI with an aluminum (Al) wire together. This sensor is simple, cost-effective and temperature insensitive, and it does not have the intrinsic magnetic saturation and hysteresis effect as it does not consist of any magnetic material. The Ampere force is generated by an electrical current flowing through the Al wire in a perpendicular magnetic field, which leads to the curvature of the Al wire and the PCF. Because the cladding mode of the PCF with a large mode field diameter is very sensitive to the curvature, this magnetic field sensor can realize a high sensitivity of 32.4 pm/mT when 100 mA electrical current is applied in our experiment. If we increase the applied electrical current, higher magnetic field sensing sensitivity and a minimal detectable magnetic field of less than 0.1 mT can be realized easily. Finally, we have to say that a similar sensor is possibly realized by attaching the Al wire to other fiber device, for example, a standard fiber Bragg grating (FBG) [21]. However a standard FBG sensor is temperature sensitive and needs complex fabrication technology. In addition, a standard FBG sensor is not as sensitive as a PCFMI sensor when it bends under the Ampere force because a standard FBG only includes

* Corresponding author.

E-mail address: feixu@nju.edu.cn (F. Xu).

core modes (insensitive to bend) while a PCFMI includes core and cladding modes.

2. Fabrication and principle

In our experiment, we used a commercial single mode PCF (LMA-8 NKT Photonics) to fabricate the PCFMI. This LMA-8 PCF includes a solid core surrounded by six rings of air holes. The core diameter, the average diameter of air holes and the average separation between the air holes are $8.4 \mu\text{m}$, $2.17 \mu\text{m}$ and $5.3 \mu\text{m}$, respectively. Initially, the PCFMI was fabricated by fusion splicing a 18 mm-long PCF between two standard single mode fibers (SMFs) with a commercial fusion splicer. In the fusion splicing region, about several hundred micrometers long air holes of the PCF collapsed completely. Then we kept the PCFMI and the Al wire straight, and we stucked the SMF sections of the PCFMI to the Al wire with glue. But we did not stick the PCF section to the Al wire because the cladding mode of PCF would be leaky with glue as the refractive index of the glue is higher than that of fiber. Finally, the bonding PCFMI and the Al wire were fixed with two holders. In the final process, we kept the PCFMI and the Al wire between the two holders a little slack without stress so that the PCF and the Al wire can bend more easily when the Ampere force is applied. We can further encapsulate the sensor device to keep long-term mechanical stability.

The schematic diagram of the experimental setup used for magnetic field sensing measurement is shown in Fig. 1(a). The broadband amplified spontaneous emission (ASE) source (1525–1610 nm) and the Ando AQ6317B optical spectrum analyzer (OSA) were used during the whole experiment to detect the interferometric behavior of the PCFMI. The glue is highlighted in yellow in Fig. 1(a) to show it more clearly while in fact the thickness of the glue was negligible and the Al wire was very close to the PCFMI. The electromagnet was connected to a control power supply. We used an Al wire instead of a copper wire because Al wire is much softer than copper wire and is easier to bend when the Ampere force is applied. The Al wire length in the magnetic field section is about 10 cm and the sensitivity will be higher if the Al wire is longer.

Fig. 1(b) shows the schematic diagram of the modal interference of the PCFMI. When the light transmits from the SMF to the collapsed PCF region, the SMF fundamental mode diffracts and excites core and cladding modes in the PCF section with different propagation constants [15–18]. Thus the modes accumulate a phase difference before they propagate to the other collapsed PCF region. Then the modes will further diffract and will be recombined through the

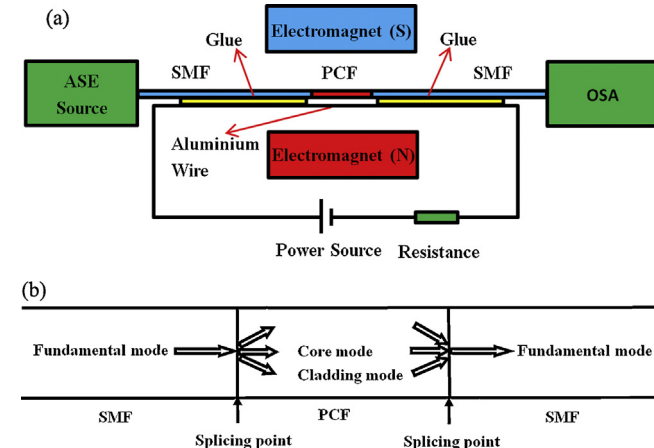


Fig. 1. (a) Schematic diagram of the experimental setup used for magnetic field sensing measurement. (b) Schematic diagram of the modal interference of the PCFMI.

filtering of the subsequent SMF. In fact many different cladding modes may be excited in the PCF and the transmission spectrum is the result of multiple-mode interference. But in order to simplify the analysis, we can only consider a cladding mode and a core mode. Therefore the transmission spectrum can be expressed with the following two-beam optical interference equation [15–18]:

$$I_{to} = I_{co} + I_{cl} + 2\sqrt{I_{co}I_{cl}} \cos\left(2\pi\Delta n_{ef}\frac{L}{\lambda}\right) \quad (1)$$

where I_{to} is the total transmission optical intensity, and I_{co} and I_{cl} are the optical intensities of the core and cladding modes, respectively. Δn_{ef} is the effective refractive indices difference between core and cladding modes. L is the PCF length and λ is the wavelength. From Eq. (1), we can see the maxima of transmission optical intensity will appear when $2\pi\Delta n_{ef}L/\lambda = 2m\pi$, where m is an integer. Therefore the transmission spectra exhibit peaks at wavelengths given by $\lambda_m = \Delta n_{ef}L/m$.

With a perpendicular magnetic field applied by the electromagnet, an electrical current flowing through the Al wire will generate Ampere force to lead to the curvature of the Al wire and the PCF. And a corresponding strain will also be induced in the PCF. Therefore three factors (curvature induced Δn_{ef} variation, strain induced Δn_{ef} variation and curvature induced L variation) together lead to the λ_m shift. If we define the group refractive index n_g as [22]

$$n_g = n_{ef} - \lambda \cdot \frac{\partial(n_{ef})}{\partial\lambda} \quad (2)$$

the theoretical λ_m shift can be expressed by [23]

$$\begin{aligned} \Delta\lambda_m = & \left(\frac{\lambda}{\Delta n_{ef} - \Delta n_g} \cdot \frac{\partial(\Delta n_{ef})}{\partial R} \right) \cdot \Delta R \\ & + \left(\frac{\lambda}{\Delta n_{ef} - \Delta n_g} \cdot \frac{\partial(\Delta n_{ef})}{\partial\varepsilon} \right) \cdot \Delta\varepsilon + \left(\frac{\lambda(\Delta n_{ef})}{L(\Delta n_g)} \cdot \frac{\partial L}{\partial R} \right) \cdot \Delta R \end{aligned} \quad (3)$$

where Δn_g is the group refractive indices difference between core and cladding modes, R is the curvature radius and ε is the strain. As the cladding mode of the PCF with a large mode field diameter is very sensitive to the curvature while the core mode of the PCF is insensitive, the curvature induced Δn_{ef} variation (the first item in Eq. (3)) plays a leading role for the λ_m shift, which can be utilized to detect the magnetic field accurately.

3. Experiment results

Fig. 2(a) shows the transmission spectra of the sensor under different magnetic field when 100 mA electrical current is applied. From Fig. 2(a), we can see different peaks and valleys show different magnetic field sensing properties. Some peaks and valleys are sensitive to magnetic field variation while other peaks and valleys are not so sensitive. We think this is because many different cladding modes are excited in the PCF and some cladding modes with larger mode field diameters are more sensitive to the curvature of the PCF while some other cladding modes with smaller mode field diameters are not so sensitive.

Fig. 2(b) shows the relationship between the resonant dip wavelength and magnetic field in ascending and descending directions. As the last valley shown in Fig. 2(a) is the most sensitive to magnetic field variation, we select it to detect the magnetic field magnitude here. From Fig. 2(b), we can see the results in ascending and descending directions both keep good linearity and are in good agreement with each other. The maximum deviation is 0.016 nm at the magnetic field of 45 mT, which may result from the fitting error of OSA data because the spectral data shown are based on fitting performance on raw data recorded on the OSA. In fact, the maximum deviation should be same as the OSA resolution 0.02 nm. Through calculation, the average magnetic field sensing sensitivity

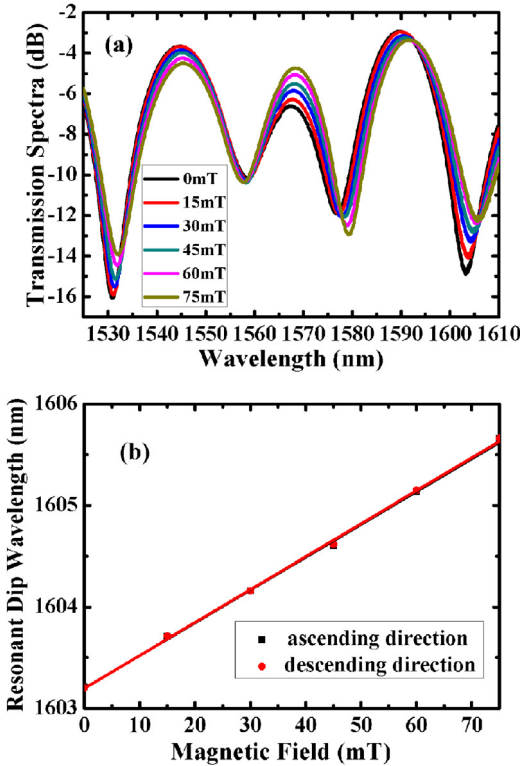


Fig. 2. (a) Transmission spectra of the sensor under different magnetic field when 100 mA electrical current is applied. (b) Relationship between the resonant dip wavelength and magnetic field in ascending and descending directions.

is 32.4 pm/mT in a perpendicular 100 mA electrical current. Considering the 0.02 nm resolution of the OSA, the minimal detectable magnetic field is about 0.6 mT. Obviously if we increase the applied electrical current, higher magnetic field sensing sensitivity can be realized. For example, we only need to increase the applied electrical current to over 600 mA and a minimal detectable magnetic field of less than 0.1 mT can be realized easily. So this proposed sensor can have potential application in detecting the geomagnetic field as the geomagnetic field magnitude is about 0.05–0.06 mT.

In our experiment, we also keep the magnetic field constant and detect the electrical current variation. Fig. 3(a) shows the transmission spectra of the sensor under different electrical current when 75 mT magnetic field is applied. The spectra in Fig. 3(a) are similar with the spectra in Fig. 2(a). Because the minimal output electrical current of the electrical power source is 100 mA, we shunt nine Al wire outside the magnetic field with the original Al wire in parallel to detect lower electrical current.

Fig. 3(b) shows the relationship between the resonant dip wavelength and electrical current in ascending and descending directions. We also select the last valley shown in Fig. 3(a) to detect the electrical current magnitude here as it is the most sensitive. From Fig. 3(b), we can see the results in ascending and descending directions also keep good linearity and the average electrical current sensing sensitivity is 25.2 pm/mA in a perpendicular 75 mT magnetic field. Considering the 0.02 nm resolution of the OSA, the minimal detectable electrical current is about 0.8 mA. But the repeatability of the results in ascending and descending directions are not as good as that in Fig. 2(b) and the maximum deviation is 0.0838 nm at the electrical current of 60 mA. We think this is reasonable because the precision of the electrical power source is low. When we increase and decrease the electrical current to 60 mA, the actual electrical current may be 60 ± 5 mA as the electrical current precision in a single Al wire is 10 mA, therefore the maximum

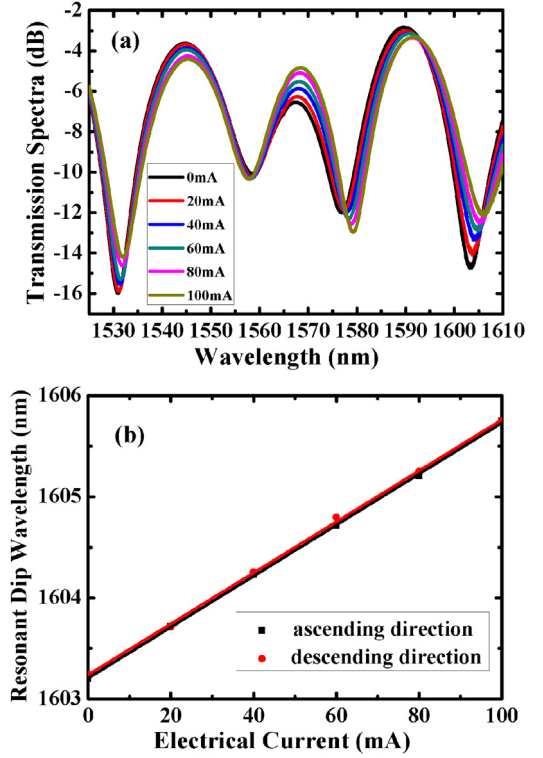


Fig. 3. (a) Transmission spectra of the sensor under different electrical current when 75 mT magnetic field is applied. (b) Relationship between the resonant dip wavelength and electrical current in ascending and descending directions.

possible error is as high as 0.252 nm. Similarly, if we increase the applied magnetic field, higher electrical current sensing sensitivity and a minimal detectable electrical current of less than 0.1 mA can also be realized easily.

It is well known that an electrical current in a perpendicular magnetic field generates an Ampere force which can be expressed by

$$F_H = I \cdot H \cdot L_H \quad (4)$$

where F_H is the Ampere force, I is the electrical current, H is the magnetic field, and L_H is the length of the electrical current experiencing the perpendicular magnetic field. From Eq. (4), we can see Ampere force is proportional to the product of the I and H . Therefore the resonant dip wavelength should be linear with the product of I and H in theory. In order to quantitatively compare the sensor sensitivity, we combine the data in Figs. 2(b) and 3(b) together and

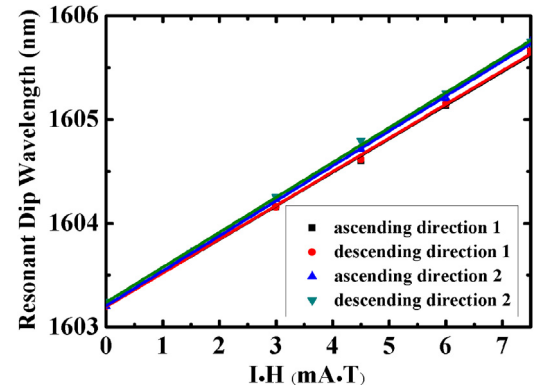


Fig. 4. Relationship between the resonant dip wavelength and $I \cdot H$ in ascending and descending directions.

draw the relationship between the resonant dip wavelength and $I \cdot H$, as shown in Fig. 4. All the results keep good linearity and the average sensitivity is about 330.3 pm/mAT. As the resolution of the OSA is 0.02 nm, the minimal detectable $I \cdot H$ is 0.06 mAT. In Fig. 4, the maximum deviation is 0.1955 nm at the $I \cdot H$ of 4.5 mAT. And this deviation is also mainly due to the low precision of the electrical power source.

4. Conclusion

In summary, a novel Ampere force based PCF magnetic field sensor is proposed and demonstrated by bonding a PCFMI with an Al wire together. The principle of the PCFMI is the interference among the core mode and excited cladding modes, and it has advantages of simple fabrication, low cost and temperature insensitivity compared with other types of interferometers. The Ampere force is generated by an electrical current flowing through the Al wire with a perpendicular magnetic field applied, and the Ampere force leads to the curvature of the Al wire and the PCF. As the cladding mode of the PCF with a large mode field diameter is very sensitive to the curvature, this magnetic field sensor can realize a high sensitivity of 32.4 pm/mT in a perpendicular 100 mA electrical current. Similarly, we also keep the magnetic field constant and detect the electrical current variation and the average electrical current sensing sensitivity is 25.2 pm/mA in a perpendicular 75 mT magnetic field. Higher sensitivity and a minimal detectable magnetic field of less than 0.1 mT or a minimal detectable electrical current of less than 0.1 mA can be realized by increasing the applied electrical current or increasing the applied magnetic field. And this sensor can have potential application in detecting the geomagnetic field as the geomagnetic field magnitude is about 0.05–0.06 mT. In addition, as Ampere force is proportional to the product of the I and H , this sensor can realize an average sensitivity of 330.3 pm/mAT and a minimal detectable $I \cdot H$ of 0.06 mAT. Our proposed and demonstrated sensor does not have the intrinsic magnetic saturation and hysteresis effect. Therefore the sensing range can be very large and the repeatability of the results in ascending and descending directions can be in good agreement with each other if the precision of the electrical power source is high.

Acknowledgments

This work is supported by National 973 program under contract Nos. 2012CB921803 and 2011CBA00205, National Science Fund for Excellent Young Scientists Fund (61322503) and National Science Fund for Distinguished Young Scholars (61225026). The authors also acknowledge the support from PAPD and the Fundamental Research Funds for the Central Universities.

References

- [1] A. Yariv, H.V. Winsor, Proposal for detection of magnetic fields through magnetostrictive perturbation of optical fibers, *Opt. Lett.* 5 (1980) 87–89.
- [2] G.W. Day, D.N. Payne, A.J. Barlow, J.J. Ramskov-Hansen, Faraday rotation in coiled, monomode optical fibers: isolators, filters, and magnetic sensors, *Opt. Lett.* 7 (1982) 238–240.
- [3] L. Sun, S. Jiang, J.R. Marcante, All-fiber optical magnetic-field sensor based on Faraday rotation in highly terbium-doped fiber, *Opt. Express* 18 (2010) 5407–5412.
- [4] T. Liu, X. Chen, Z. Di, J. Zhang, X. Li, Tunable magneto-optical wavelength filter of long-period fiber grating with magnetic fluids, *Appl. Phys. Lett.* 91 (2007) 121116.
- [5] J. Dai, M. Yang, X. Li, H. Liu, X. Tong, Magnetic field sensor based on magnetic fluid clad etched fiber Bragg grating, *Opt. Fiber Technol.* 17 (2011) 210–213.
- [6] P. Zu, C.C. Chan, W.S. Lew, Y. Jin, Y. Zhang, H.F. Liew, L.H. Chen, W.C. Wong, X. Dong, Magneto-optical fiber sensor based on magnetic fluid, *Opt. Lett.* 37 (2012) 398–400.
- [7] X. Li, H. Ding, All-fiber magnetic-field sensor based on microfiber knot resonator and magnetic fluid, *Opt. Lett.* 37 (2012) 5187–5189.
- [8] C.L. Tien, C.C. Hwang, H.W. Chen, W.F. Liu, S.W. Lin, Magnetic sensor based on side-polished fiber Bragg grating coated with iron film, *IEEE Trans. Magnet.* 42 (2006) 3285–3287.
- [9] M. Yang, J. Dai, C. Zhou, D. Jiang, Optical fiber magnetic field sensors with TbDyFe magnetostrictive thin films as sensing materials, *Opt. Express* 17 (2009) 20777–20782.
- [10] G.N. Smith, T. Allsop, K. Kalli, C. Koutsides, R. Neal, K. Sugden, P. Culverhouse, I. Bennion, Characterisation and performance of a Terfenol-D coated femtosecond laser inscribed optical fibre Bragg sensor with a laser ablated microslot for the detection of static magnetic fields, *Opt. Express* 19 (2011) 363–370.
- [11] Y. Dai, M. Yang, G. Xu, Y. Yuan, Magnetic field sensor based on fiber Bragg grating with a spiral microgroove ablated by femtosecond laser, *Opt. Express* 21 (2013) 17386–17391.
- [12] S. Jin, H. Mavoori, R.P. Espindola, L.E. Adams, T.A. Strasser, Magnetically tunable fiber Bragg gratings, in: Proc. OFC'99, San Diego, CA, ThJ2, 1999, pp. 135–137.
- [13] L. Cheng, Z. Guo, J. Han, L. Jin, B.O. Guan, Ampere force based magnetic field sensor using dual-polarization fiber laser, *Opt. Express* 21 (2013) 13419–13424.
- [14] P. Russell, Photonic crystal fibers, *Science* 299 (2003) 358–362.
- [15] J. Villatoro, V. Finazzi, V.P. Minkovich, V. Pruneri, G. Badenes, Temperature-insensitive photonic crystal fiber interferometer for absolute strain sensing, *Appl. Phys. Lett.* 91 (2007) 091109.
- [16] R. Jha, J. Villatoro, G. Badenes, V. Pruneri, Refractometry based on a photonic crystal fiber interferometer, *Opt. Lett.* 34 (2009) 617–619.
- [17] S.J. Qiu, Y. Chen, J.L. Kou, F. Xu, Y.Q. Lu, Miniature tapered photonic crystal fiber interferometer with enhanced sensitivity by acid microdroplets etching, *Appl. Opt.* 50 (2011) 4328–4332.
- [18] S.J. Qiu, Y. Chen, F. Xu, Y.Q. Lu, Temperature sensor based on an isopropanol-sealed photonic crystal fiber in-line interferometer with enhanced refractive index sensitivity, *Opt. Lett.* 37 (2012) 863–865.
- [19] H.V. Thakur, S.M. Nalawade, S. Gupta, R. Kitture, S.N. Kale, Photonic crystal fiber injected with Fe_3O_4 nanofluid for magnetic field detection, *Appl. Phys. Lett.* 99 (2011) 161101.
- [20] R. Gao, Y. Jiang, S. Abdelaziz, All-fiber magnetic field sensors based on magnetic fluid-filled photonic crystal fibers, *Opt. Lett.* 38 (2013) 1539–1541.
- [21] J. Gong, C.C. Chan, M. Zhang, W. Jin, J.M.K. MacAlpine, Y.B. Liao, Fiber Bragg grating current sensor using linear magnetic actuator, *Opt. Eng.* 41 (2002) 557–558.
- [22] T. Allsop, L. Zhang, I. Bennion, Detection of organic aromatic compounds in paraffin by a long-period fiber grating optical sensor with optimized sensitivity, *Opt. Commun.* 191 (2001) 181–190.
- [23] T. Allsop, A. Gillooly, V. Mezentsev, T. Earthgowl-Gould, R. Neal, D.J. Webb, I. Bennion, Bending and orientational characteristics of long period gratings written in D-shaped optical fiber, *IEEE Trans. Instrument. Meas.* 53 (2004) 130–135.

Biographies

Sun-jie Qiu is a graduate student in College of Engineering and Applied Sciences and National Laboratory of Solid State Microstructures, Nanjing University, Nanjing 210093, PR China. His research is concentrated on optical fiber sensors.

Qi Liu is a graduate student in College of Engineering and Applied Sciences and National Laboratory of Solid State Microstructures, Nanjing University, Nanjing 210093, PR China. His research is concentrated on optical fiber sensors.

Dr. Fei Xu received the Ph.D. degree from Optoelectronics Research Centre at University of Southampton, UK in 2008. He is now a professor of the College of Engineering and Applied Sciences and the National Laboratory of Solid State Microstructures, Nanjing University, China. He has published over 80 peer-reviewed papers on optoelectronic materials and devices. His current research interests are fiber sensor and laser, nonlinear optics and optomechanical effect.

Dr. Yan-qing Lu is now a professor of the College of Engineering and Applied Sciences and the National Laboratory of Solid State Microstructures, Nanjing University, China. As an IEEE senior member, he owns 15 US and China patents. He has published over 100 peer-reviewed papers on opto-electronic materials and devices. His current research interests include nano-photonics, fiber optics and liquid crystal devices.